LATVIAN JOURNAL OF PHYSICS AND TECHNICAL SCIENCES
2008, N 2
DOI: 10.2478/v10047-008-0008-4

NEUTRON BRAGG DIFFRACTION ON A BENT SILICON SINGLE CRYSTAL EXCITED BY ULTRASOUND

E. Raitman, V. Gavrilov,
M. Brezgunov and D. Mjasiscev

Institute of Physical Energetics ,
21 Aizkraukles Str., Riga, LV-1006, LATVIA

The neutron Bragg diffraction on a bent silicon monocrystal excited by ultrasound was investigated. It is shown that for perfect crystal the relative diffraction intensity is proportional to the acoustic wave amplitude w. The calibration parameters between the generator voltage and acoustic wave amplitude were derived assuming $w = (2.3\pm0.3)\cdot10^{-2}$ Å/V. To explain the results, a modified Penning–Polder–Kato model was applied. In a bent crystal, owing to ultrasound, transitions between the sheets of a dispersion surface take place. This leads to various manifestations of the behaviour of the integral scattering intensity, which drastically differs from the case of a perfect crystal. The observed effects may be used for creating new types of neutron monochromators and choppers governed by the ultrasound wave amplitude as well as by the length and bending radius of the crystal.

1. INTRODUCTION

The effect of ultrasound (US) on neutron and X-ray scattering in perfect crystals has been the subject of many investigations (see, e.g. [1–3, 6–8] and [9–10, 13], respectively). Their main results could be reduced to the following. In the long-wave limit ($\lambda_s >> \tau$, where λ_s is the US wave length, τ is the extinction length), US excitation leads to increased diffraction intensity up to the kinematical limit. The US effect on the diffraction can be considered as a smooth and time-dependent lattice deformation [14]. When $\lambda_s << \tau$, the US mixes the states corresponding to different sheets of the dispersion surfaces (DSs), producing self-intersection points and a new area of the total reflection governed by US. This results in a new type of oscillations that depend on the acoustic wave amplitudes [3].

In deformed crystals, which are of great practical interest, the impact of US on diffraction has been investigated much less. The authors of [4, 7–9] report the results of theoretical and experimental data for the behaviour of neutrons and X-rays [11, 12] at Laue's diffraction in deformed silicon single crystals under high-frequency ($\lambda_s << \tau$) excitations. Their analysis has shown that in smoothly deformed Si crystals the US effect is expressed in violation of the adiabatic conditions for the movement of tie points on the dispersion surfaces. Owing to this, a drastic decrease in the diffraction intensities was observed for low amplitudes of acoustic waves. With the amplitude increasing, the diffraction intensity also in-

creases, reaching the kinematical limit. In absolute values, the US effect is much stronger manifested in diffraction on a deformed crystal than on the ideal one. A substantial role is played by multiphonon processes [4, 6–8]. The presence of static strains leads to the appearance of a new type of oscillations depending on the value of deformation gradient [4].

The aim of the present work was to continue our previous investigations into the Laue diffraction and to study the impact of high-frequency ultrasound on neutron scattering in the case of Bragg's reflection from a bent silicon monocrystal.

2. EXPERIMENTAL

As a sample, a dislocation-free silicon monocrystal 0.6×6×12 cm^3 in size was taken. The layout of a bent crystal and the scattering geometry are shown in Fig. 1. In such a Bragg-symmetry geometry, reflections (220) and (440) were measured simultaneously, employing a simple one-crystal diffractometer and the TOF method. The sample was bent using an ordinary so-called four-point bending device (Fig. 1). The sag of span h was measured by a micrometer. It is easy to show that the curvature radius R is reciprocally proportional to h as $R \approx L^2/8h$, where L=12 cm is the sample length.

In the experiments, a transverse US wave ($\mathbf{K}_s \perp \mathbf{K}_0$, **H**; **W**||**H**) was excited in the crystal with a $LiNbO_3$ piezotransducer glued on the sample by salol. The first harmonic (ν_s = 26.5 MHz) was used to make possible the work near the neutron acoustic resonance frequency, ν_{res} = 25.8 MHz.

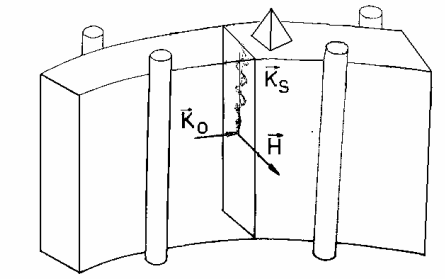

Fig. 1. The general view of a bent scattering crystal; **H** - the vector of reciprocal lattice, $\mathbf{K}_0$ – the wave number of neutrons, $\mathbf{K}_s$ – the ultrasound wave vector.

3. RESULTS

In Fig. 2*a*, the frequency dependence of diffraction intensities is shown. It is seen that this cannot be interpreted as a one-mode US. The diffraction intensity *vs.* frequency measured stepwise with small steps is presented in Fig. 2*b* in detail, showing that in the crystal standing waves are created. This subject will be developed below in the discussion.

The most important experimental results are shown in Figs. 3–5.

Figure 3 shows typical plots of the relative diffraction intensities *vs.* the piezotransducer voltage for two reflections, (220) and (440), in the "perfect" crystal (without bending). It is seen that linear dependence is a good approximation.

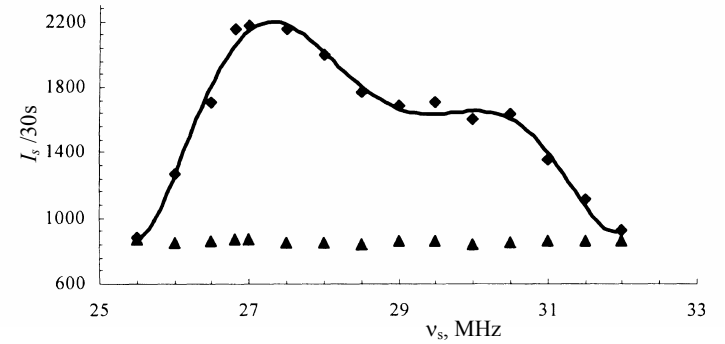

Fig. 2a. Diffraction intensity I_s *vs.* the US frequency. The lower points (▲): I_s dependence without sound. The solid curve is obtained by averaging over 3 points.

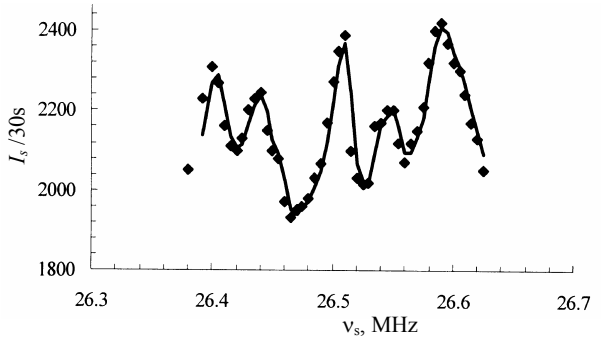

Fig. 2b. The same as in Fig. 2*a* for a narrow frequency interval of 26.3–26.7 MHz (operational mode 26.5 MHz).

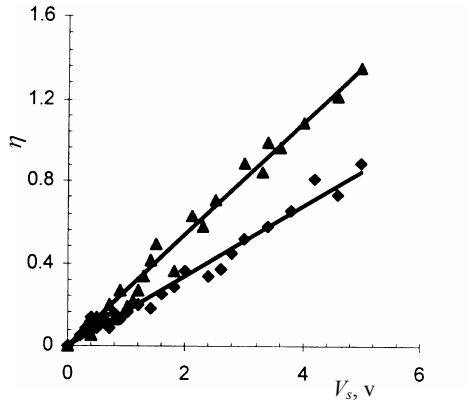

Fig. 3. Relative changes of the diffraction intensities $\eta = (I_s - I_0)/I_0$ for perfect crystal for two reflections: (440) – ▲, (220) – ♦.

Figures 4*a–c* display typical plots of the diffraction intensity I_{sd} *vs.* piezotransducer voltage at different R values for (440) reflection. As distinct from the linear dependences $I_s = f(v_s)$ in Figs. 3*a,b*, for the bent crystal a noticeable decrease in the diffraction intensity is observed already at low ultrasound amplitudes, reaching 50% for R = 60 m (Fig. 4*b*). In Fig. 4*a* it is seen that more than one phonon participate in this phenomenon. With R decreasing, the minima on the curves are moving towards large V_s and become worse resolved (Fig. 4*c*).

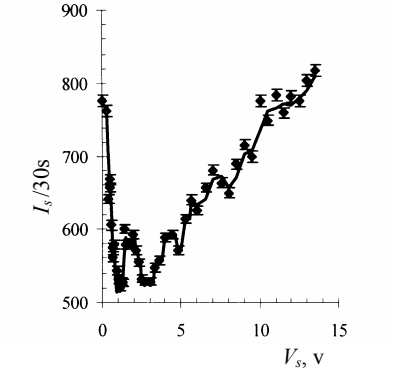

Fig. 4a. Diffraction intensity I_{ds} *vs.* piezotransducer voltage V_s for (440) reflection with R= 600m (h = 0.3μm). A two-phonon scattering is clearly seen.

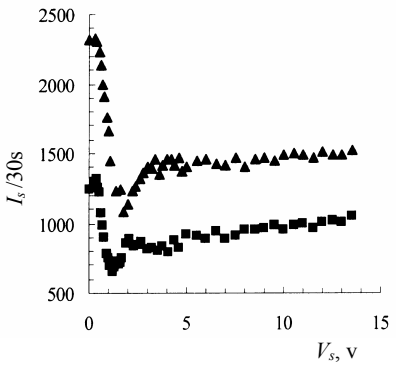

Fig. 4b. The same as in Fig. 4*a* for R=180 m (■) and R=60 m (▲).

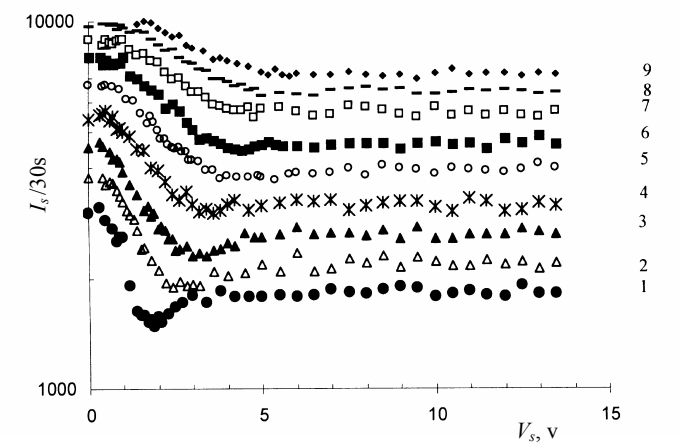

Fig. 4c. The same as in Figs. 4 *a,b* for different bending radii: *1* – 36 m, *2* – 25.7 m, *3* – 20 m, *4* – 15m, *5* – 11.3m, *6* – 9m, *7* – 7.2 m, *8* – 6m, *9* – 5.1m; λ_n = 0.096 nm; I_s is shown in the logarithmic scale.

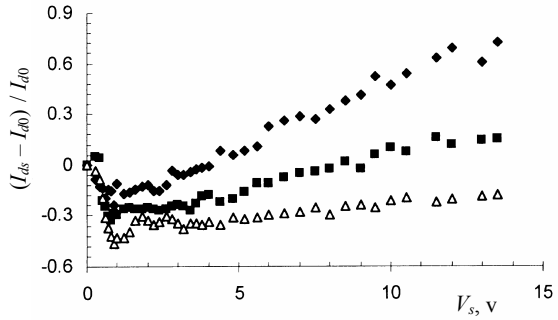

Fig. 5. Relative diffraction intensity $\eta = (I_{ds} - I_{d0}) / I_{d0}$ *vs.* piezotransducer voltage for (220) reflection and for three different bending radii: (Δ) – R = 60 m, (■) – R = 180 m, (♦) – R = 600 m. I_{ds} is the diffraction intensity for a deformed crystal excited with US; I_{d0} is the same with sound switched off; λ_n = 0.192 nm.

Figure 5 shows that the position of minima of parameter η is moving towards higher V_s with R decreasing.

In Figs. 4 and 5 it is seen that the position of minima depends both on the flexure radius R and the US wave amplitudes, $V_s \sim w$; however, the maximum of "depression" $\eta \approx 0.5$ is connected with neutron wave length λ_n and reflection numbers only slightly.

4. DISCUSSION

A correct consideration of simultaneous influence of both the types of crystalline lattice deformation – static (bending) and dynamic (displacement of atoms in US wave) ones – on the diffraction of neutrons in Laue's geometry was given in works [3, 11], where numerically (by the method of successive approximations) and, for separate cases, analytically a modified Takagi–Taupin equation was solved; in [5], for this purpose Green's functions were employed. In the case of Bragg's geometry, the mathematical problem becomes much more complicated owing to specific boundary conditions, and, to our knowledge, has so far no analytical solution. Below, within the limits of the neutron scattering dynamic theory, a semi-phenomenological model is considered, which, nevertheless, not only gives a qualitative explanation of the experimental results but, in some cases, allows numerical characteristics to be obtained. Two cases are considered: of perfect crystal and of deformed crystal.

Perfect crystal

Most theoretical calculations have been done for the case of a coherent (one-mode) US wave. However, in our case one-mode US waves cannot be excited; from Fig. 2*a* it is seen that the US field is incoherent, so the distribution of frequency spectrum could be described in very broad limits. Nevertheless, as shown in [17], under our experimental conditions the one-mode model is not needed for correct interpretation of results.

For standing waves the relation $T = i\,\lambda_s/2$ (where i is the whole number of transverse US half-waves, λ_s is the neutron wave length, and T is the distance covered by US waves) will hold. Knowing T and the distance between the maxima (minima) $\Delta v_s = v_{si} - v_{s(i \pm 1)}$, we can determine sound velocity $v_{s.}$ in the direction [110] parallel to the scattering plane. Defining Δv_s from the dependences shown in Fig. 2*b*, where $\Delta v_s = (0.049 \pm 0.008)$ MHz, one can see that i is equal to 540 and $v_{s[110]} = 5.89 \cdot 10^5$ cm/s, and that this latter value is very close to the reference data of $5.85 \cdot 10^5$ cm/s [15]. Thus, the values of US wave velocities in crystals can be determined using the neutron and X-ray diffraction technique. This statement is also valid for slightly deformed crystals.

Since the measurements were made with the frequency exceeding the neutron–acoustic resonance v_{res}, the linear dependences shown in Fig. 3 may be expected. According to [3], the resonance frequency for a neutron is defined by the expression:

$$\nu_{res} \approx (v_n \cos\Theta_B)/\tau\,, \tag{1}$$

where Θ_B and v_n is the Bragg angle and the neutron velocity, respectively, and τ is the extinction length.

Expression (1) is valid for our case when the angle between **H** and $\mathbf{K}_s$ is equal to 90°. From (1) it follows that ν_{res} = 25.3 MHz [16], which is below our operational frequency ν = 26.5 MHz. Taking into account the Debay–Waller factor, the ν_{res} value is the same for all observed reflections ((220), (440), etc.).

At $\nu > \nu_{res}$ a mixing of ground states occurs, and on the dispersion surfaces new energy gaps $\Delta\mathbf{k}_s$ arise (see Fig. 6), which in the Bragg geometry correspond to the additional regions of total reflection. The absorption (emission) of the US phonon displaces the dispersion surface of a neutron by $\delta\mathbf{q}$:

$$\delta\mathbf{q} = \nu_s / (v_n \cos\Theta_B) \pm \mathbf{k}_s , \tag{2}$$

which leads to a linear growth in the diffraction intensity depending on the amplitude of the US wave.

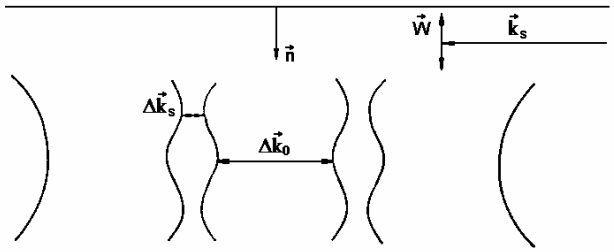

Fig. 6. Schematic sketch of the dispersion surfaces for Bragg's geometry in the presence of US excitation; **n** is the normal to the surface (the scattering plane) [18].

As shown in [3], in the case of $\nu > \nu_{res}$ the changes of relative diffraction intensities can be determined as

$$\eta = (I_s - I_0)/I_0 \approx 2|Hw| , \tag{3}$$

and, assuming $Hw = cV_s$ from the plots of Fig. 3, one can obtain calibration parameter c and estimate the US wave amplitudes w: $c_{(220)}$ = 0.167 and $c_{(440)}$ = 0.290, from where $w = (2.3 \pm 0.3)\cdot 10^{-2}$ Å/V could be derived.

Deformed crystal

For the Laue diffraction in smoothly deformed crystals the problem was analysed in [4]. The model described in this work is applicable, as will be shown, also for the case of Bragg's geometry. As distinguished from the scheme of Fig. 6 that shows for the whole perfect crystal a unitary dispersion surface, in the Penning–Polder–Kato model [17] to each point of a bent crystal an own two-sheet dispersive surface corresponds, and the neutron is moving adiabatically inside the crystal without transitions of the excited point between the DS sheets. The role of ultrasound in this model consists in resonant suppression of the adiabatic movement of tie points.

The one-phonon absorption corresponds to path 1–2–6–7–8 of the tie point along the dispersion surface (Fig. 7). The neutron incident on the crystal excites points 1 and 8 on the DS. In the absence of ultrasound, point 1 travels path 1–2–3–4 and passes into the state corresponding to a diffracted wave. Point 8 makes no contribution to the diffraction. When US is switched on, the movement of point 8 is not disturbed. As concerns point 1, it can reach state 4 by two ways: a) 1–2–6–7–3–4

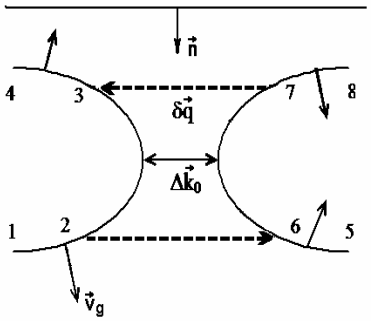

Fig. 7. Dispersion surface of neutrons for Bragg's geometry. The broken arrows show transition of tie points from one DS sheet to another. Solid arrows denote the direction of neutron group velocities for adiabatic motion of the tie point along the DS in a deformed crystal.

or b) 1–2–3–4. If the probability for the excitation point to remain on DS sheets at points 2, 3 6, and 7 is P and the probability to pass onto another DS sheet owing to the US disturbance is M (P+M = 1), then the probability of the former process is equal to M^2, the probability of the latter process is equal to P^2, and the change in the relative diffraction intensity will be

$$\eta = (I_{ds} - I_{d0}) / I_{d0} = P^2 + M^2 - 1 = -2MP < 0 . \quad (4)$$

The probability of transition for the excitation point in the case of Laue's diffraction is approximately described as

$$M \approx 1 - \exp[-\pi (Hw)^2 / 2B], \quad (5)$$

where B is the deformation gradient.

Using expressions (4) and (5), for the position of $(Hw)_{\min}$ depending on the bending radius we will have:

$$(Hw)_{\min} = aR^{-0.5}, \quad (6)$$

The deformation gradient is inversely proportional to the bending radius ($B \sim 1/R$).

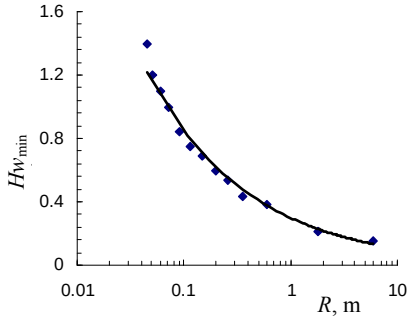

Fig. 8. Position of the maximum decrease in the diffraction intensities $Hw_{\min}$ (see Figs. *4a–c*, 5) *vs.* bending radius R for two reflections: (♦) – (220), (■) – (440) (R is shown in logarithmic scale). The solid curve fits the expression $(Hw)_{\min} = 2.04 \cdot R^{-0.44}$; Hw is calculated using calibration parameter c for perfect crystal.

Therefore, the modified Penning–Polder–Kato model describes satisfactorily some peculiarities of the Bragg scattering of neutrons on a bent silicon crystal. However, this model fails to describe the dependence of the absolute value of diffraction intensity dip $|\eta_{max}|$ on the bending radius shown in Fig. 9. This value is close to 0.5 – as it follows from formula (4) and is reached at R = 20–60 m, after which it decreases smoothly. Possibly, this is connected with neglect of multi-phonon processes.

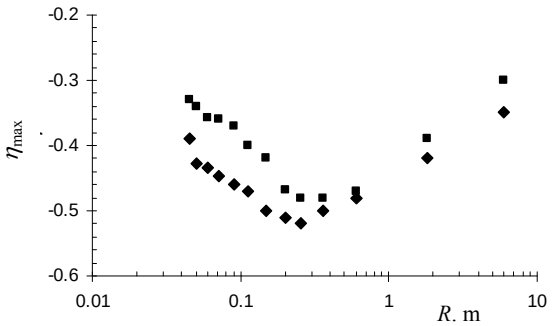

Fig. 9. The maximum relative changes in the diffraction intensity (the dip) *vs*. the bending radius for neutrons with two wave lengths:(■) – 1.31 Å, (♦) – 1.92 Å.

5. CONCLUSION

It has been shown that in the case of Bragg's geometry of neutron scattering the diffraction differs noticeably from Laue's one. However, a modified Penning–Polder–Kato model can successfully be applied for explanation of the experimental data. In a bent crystal, transitions between the sheets of a dispersion surface take place. This leads to various manifestations of the behaviour of the integral scattering intensity, which drastically differs from the case of a perfect crystal. A set of the diffraction intensity minima connected with ultrasound phonon–neutron interactions has been observed. Their depth and position depend on the bending radius and, at the same time, on the amplitudes of ultrasound wave.

The observed effects may be used for creating new types of neutron monochromators and choppers governed by the ultrasound wave amplitude as well as by the length and bending radius of the crystal.

REFERENCES

1. Köhler, R. , Möhling, W. & Peibst, H. (1974). *Phys. Status Solidi (b)* **61**, 439.
2. Mikula, P. Lukas, P. & Kulda J. (1992) *Acta Cryst. A*. **48**, 72.
3. Iolin, E., Zolotoyabko, E., Raitman, E. & Kuvaldin., B. (1986). *Zh. Eksp. Teor. Fiz*. **91**, 2132.
4. Iolin, E., Raitman, E., Kuvaldin, B., Gavrilov, V. & Zolotoyabko, E. (1988). *Zh. Eksp. Teor. Fiz*. **94**, 218.
5. Chukhovskii, F.N., Nosik, V.L. & Iolin, E. M. (1993). *Zh. Eksp. Teor. Fiz.* **104**, 2452.
6. Iolin, E., Farago, B., Raitman, E.& Mezei, F. (1998). *Physica B* **241-243** 1213.
7. Felber, J., Gähler, R., Rauch, C. & Golub, R. (1996). *Phys. Rev. A* **53** 1 319.
8. Aksenov,V., Gavrilov,V., Nikitenko,Yu., Progliado,V., & Raitman E. (2004). *Latv. J. Phys. Tech. Sci*. (3), 55.

9. Assur, K. & Entin, I. (1982). *Fiz. Tverd. Tela* **26**, 2122.
10. Roshchupkin, D., Irzhak, D., Tucoulou, R. & Buzanov, O. (2003). *J. Appl. Phys.* **94**, (10), 6692.
11. Iolin, E., Raitman, E., Gavrilov, V, Kuvaldin, B. & Rusevich, L. (1995). *J. Phys. D.: Appl. Phys*.28, A281.
12. Gavrilovs, V., Mjasishchevs, D., & Raitmans, E. (2005). *Latv. J. Phys. Tech. Sci*., (1), 3.
13. Zolotoyabko, E. (1999) *Nucl. Instr. Methods,* **B131**, 410.
14. 14 Благов, А.Е., Ковальчук, М.В., Кон, В.Г., Писаревский, Ю.В. (2006). *Кристаллография,* **51,** (5), 1.
15. *Акустические кристаллы*. Справочник. (1982), М.: Наука.
16. Penning, P. (1966) *Philips Res. Rep.,* suppl., **5**, 1; Kato, N. (1964) *J. Phys. Soc. Jpn.* **19,** 67.
17. Iolin, E., Rusevich, L., Strobl, M. *et al* (2005) *Nucl. Instr. Metods*, A259, 152.

NEITRONU BREGA DIFRAKCIJA UZ IZLIEKTA SILĪCIJA MONOKRISTĀLA, KAS IEROSINĀTS AR ULTRASKAŅU

E. Raitmans, V. Gavrilovs, M. Brezgunovs, D. Mjasiscevs

K o p s a v i l k u m s

Rakstā pētīta neitronu Brega difrakcija uz izliekta silīcija monokristāla, kas ierosināts ar ultraskaņu. Parādīts, ka ideālam kristālam difrakcijas relatīvā intensitāte ir proporcionāla viļņu akustiskai amplitūdai w. Ģeneratora sprieguma un viļņu akustisko amplitūdu kalibrēšanas parametri iegūti, dodot $w = (2.3\pm0.3)\cdot10^{-2}$ Å/V.

Lai izskaidrotu iegūtos rezultātus, pielietoja modificētu Penninga–Poldera–Kato modeli. Saskaņā ar šo modeli uz izliekta kristāla ultraskaņas ietekmē notiek pārejas starp dispersijas virsmas plāksnēm. Tas rada pilnās izkliedes intensitātes dažādas uzvedības parādīšanos, kas būtiski atšķiras no ideālā monokristāla. Iegūtos efektus var izmantot jaunu neitronu monohromatoru un pārtraucēju tipu izveidošanā, kuri darbojas atkarībā no ultraskaņas viļņu amplitūdas, kā arī no kristāla izliekuma rādiusa un tā garuma.

04.04.2008.